

ARTICLE

Physiologically Based Pharmacokinetic Approach to Determine Dosing on Extracorporeal Life Support: Fluconazole in Children on ECMO

Kevin M. Watt^{1*}, Michael Cohen-Wolkowicz¹, Jeffrey S. Barrett², Michael Sevestre³, Ping Zhao⁴, Kim L.R. Brouwer⁵ and Andrea N. Edginton⁶

Extracorporeal life support (e.g., dialysis, extracorporeal membrane oxygenation (ECMO)) can affect drug disposition, placing patients at risk for therapeutic failure. In this population, dose selection to achieve safe and effective drug exposure is difficult. We developed a novel and flexible approach that uses physiologically based pharmacokinetic (PBPK) modeling to translate results from ECMO *ex vivo* experiments into bedside dosing recommendations. To determine fluconazole dosing in children on ECMO, we developed a PBPK model, which was validated using fluconazole pharmacokinetic (PK) data in adults and critically ill infants. Next, an ECMO compartment was added to the PBPK model and parameterized using data from a previously published *ex vivo* study. Simulations using the final ECMO PBPK model reasonably characterized observed PK data in infants on ECMO, and the model was used to derive dosing in children on ECMO across the pediatric age spectrum. This approach can be generalized to other forms of extracorporeal life support (ECLS), such as dialysis.

CPT Pharmacometrics Syst. Pharmacol. (2018) 7, 629–637; doi:10.1002/psp4.12338; published online on 13 August 2018.

Study Highlights

WHAT IS THE CURRENT KNOWLEDGE ON THE TOPIC?

☑ ECLS can alter drug exposure via multiple mechanisms. Current approaches to determine dosing have important limitations.

WHAT QUESTION DID THIS STUDY ADDRESS?

☑ This study evaluated a novel approach that used PBPK modeling to translate results from benchside ECLS circuit-drug interaction experiments into bedside dosing recommendations.

WHAT DOES THIS STUDY ADD TO OUR KNOWLEDGE?

☑ This approach successfully determined fluconazole dosing in children on ECMO across the pediatric age spectrum.

HOW MIGHT THIS CHANGE DRUG DISCOVERY, DEVELOPMENT, AND/OR THERAPEUTICS?

☑ This study showed that benchside ECLS circuit-drug interaction experiments can be used to parameterize an ECLS compartment in a PBPK model and predict dosing in this vulnerable population. The study focused on a form of cardiopulmonary ECLS (i.e., ECMO), but this approach can be easily adapted to other more common forms of ECLS, such as dialysis.

Extracorporeal life support (ECLS), such as dialysis or extracorporeal membrane oxygenation (ECMO), provides an artificial organ that is life-saving for patients with organ failure. However, in treating patients on ECLS, one of the challenges is understanding and appropriately compensating for the effect of the extracorporeal circuit on drug pharmacokinetics (PKs). Drug PKs can be altered in three primary ways: (i) adsorption of drug to the various components of the device;^{1,2} (ii) increased volume of distribution due to hemodilution and physiologic changes associated with ECLS

(e.g., inflammation);^{3–5} and (iii) altered clearance due to the underlying disease or direct impact of the artificial organ.⁶ As a result, optimal dosing in this setting likely differs compared to individuals not on ECLS.

ECMO is a form of cardiopulmonary ECLS that provides lung and heart support in critically ill infants, children, and, increasingly, in adults with cardiorespiratory failure. In these vulnerable populations, the effect of ECMO on drug disposition leaves clinicians with uncertainty about the optimal dosing regimen. Historically, drug dosing on ECMO was

¹Duke Clinical Research Institute, Duke University Medical Center, Durham, North Carolina, USA; ²Sanofi-Aventis, Bridgewater, New Jersey, USA; ³Design2Code Inc., Waterloo, Ontario, Canada; ⁴Bill and Melinda Gates Foundation, Seattle, Washington, USA; ⁵Division of Pharmacotherapy and Experimental Therapeutics, UNC Eshelman School of Pharmacy, Chapel Hill, North Carolina, USA; ⁶University of Waterloo School of Pharmacy, Waterloo, Ontario, Canada. *Correspondence: Kevin M. Watt (kevin.watt@duke.edu)

determined by dedicated PK trials in patients supported with ECMO or by *ex vivo* experiments in which drug was injected into isolated ECMO circuits to quantify adsorption by the circuit.

PK trials in patients on ECMO remain the gold-standard; based on these trials, dosing recommendations for some antibiotics and sedatives were modified.^{7,8} However, there are three limitations to PK trials in this population. First, the effect of ECMO on exposure is drug specific, necessitating a trial for each drug of interest.⁹ Second, the impact of ECMO can vary by age of the patient.¹⁰ Most ECMO PK trials were conducted in infants; and it is not clear whether the results can be extrapolated to older children and adults. Third, advances in ECMO technology over time may affect drug disposition differently, which could impact dosing recommendations.¹¹ Given the differences reported in drug extraction between older components (e.g., silicone membrane oxygenators) and newer technology (e.g., polymethylpentane hollow-fiber oxygenators), it is unknown whether dosing recommendations derived from trials using the older technology can be extrapolated to patients supported with modern ECMO circuits. Consequently, PK trials require large numbers of children and may need to be repeated as ECMO technology evolves.

Circuit-drug interactions have been investigated using *ex vivo* ECMO experiments in which drug is administered to an isolated ECMO circuit.^{2,9,11} Because there is no corporeal metabolism or elimination in this system, decreases in drug concentration over time are due to either adsorption by the circuit or drug degradation. These studies are less expensive and faster than clinical trials. However, the ability to use these results to inform dosing recommendations has been limited.

Physiologically based pharmacokinetic (PBPK) models can address the limitations of traditional PK trials with

compartmental modeling by translating ECMO *ex vivo* results into dosing recommendations. PBPK models are structured to represent physiologically relevant spaces. Each virtual “organ” is parameterized with mass-balance differential equations describing the disposition of drug within the compartment. Because PBPK models are mechanistic, age-related processes of drug disposition can be incorporated into the model to predict exposure across the pediatric age spectrum. Further, the model parameters can be adjusted to account for the altered physiology associated with critical illness (e.g., decreased renal blood flow). In order to model drug exposure in patients on ECMO, an ECMO “organ” can be linked to the PBPK model and parameterized using data from *ex vivo* studies. By defining the volume, blood flows, and drug clearance of the ECMO compartment, the impact of ECMO on drug disposition can be predicted *in vivo*, and the ECMO PBPK model can be used to determine optimal dosing in this vulnerable population. Furthermore, as ECMO technology evolves, the impact of new equipment can be quantified with *ex vivo* experiments and incorporated into the ECMO compartment of the PBPK model rather than repeating the entire clinical trial to determine dosing. This novel approach to develop an optimal dosage regimen for patients on ECMO is cost effective and will decrease the number of children required for dosing trials.

The goal of this analysis was to evaluate the ECMO-PBPK approach by developing a PBPK model of fluconazole in children on ECMO. We focused on fluconazole in this population because invasive candidiasis is common, and often fatal, and treatment relies on optimal dosing.^{12,13} The final PBPK model was used to predict optimal dosing in children on ECMO across the pediatric age spectrum.

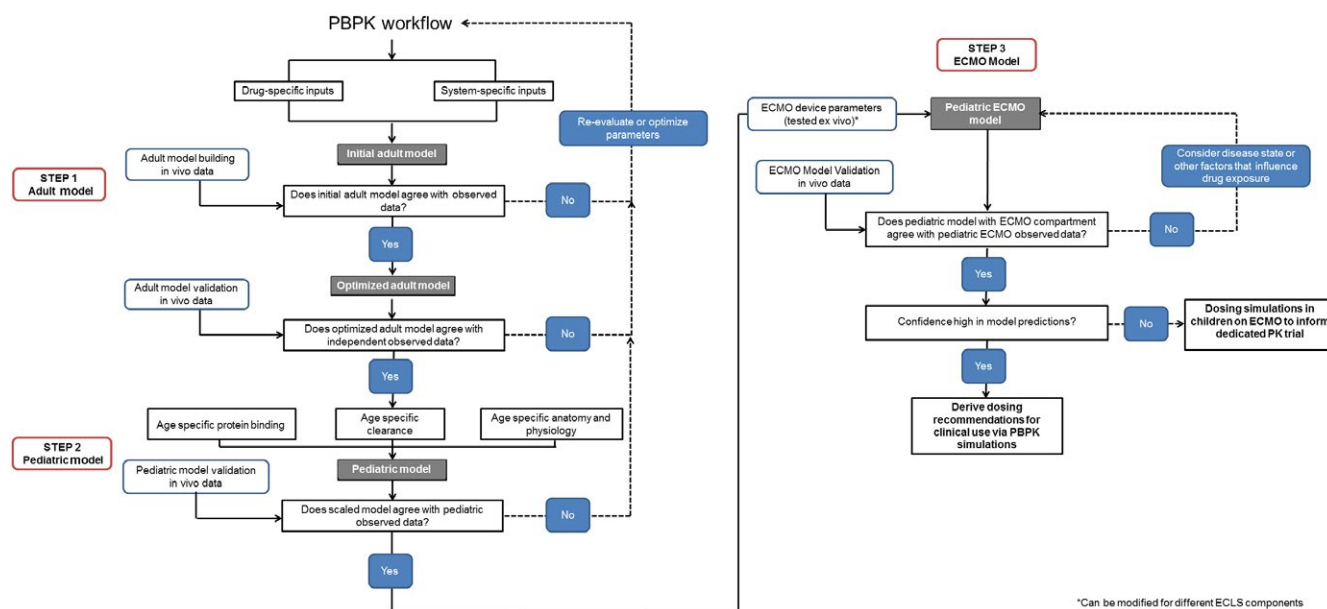


Figure 1 An iterative workflow for predicting drug pharmacokinetic (PK) in children on extracorporeal membrane oxygenation (ECMO) using physiologically based pharmacokinetic (PBPK) models. Step 1: development and validation of the adult PBPK model. Step 2: development and validation of the pediatric PBPK model. Step 3: verification and application of the pediatric ECMO PBPK model.

METHODS

Model building workflow

We built the PBPK model using an established workflow (Figure 1, Appendix S1).¹⁴ A PBPK model was first developed in adults (adult PBPK model) to gain confidence in the model structure using robust adult data before proceeding with pediatric model development. After model validation, the adult PBPK model was scaled to children (pediatric PBPK model). Once the pediatric PBPK model met acceptance criteria of model validation using clinical PK data in children not on ECMO, an ECMO compartment was added to the pediatric PBPK model to form the ECMO PBPK model. The ECMO compartment was parameterized using data from our previously published *ex vivo* study.¹⁵ The ECMO model was updated to include edema that is common in patients on ECMO.^{16,17} Model predictions in children on ECMO were evaluated using data from our ECMO Fluconazole PK trial.¹⁰

Adult PBPK model

We developed a whole-body PBPK model for fluconazole in adults using the software PK-Sim and MoBi version 7.2 (Open Systems Pharmacology Suite, www.open-systems-pharmacology.com). The PBPK model was structured with 15 organs using mass balance differential equations describing drug entering and exiting the various organ compartments. The link between physiologic spaces was the blood circulation. The model assumed a 30-year-old white man with a mean body weight of 73 kg and height of 176 cm based on population-level data from the National Health and Nutrition Examination Survey dataset.¹⁸ Based on these anthropometric measurements, organ weights, volumes, and blood flows were generated using the International Commission on Radiological Protection database.¹⁹

The distribution model assumed each organ consisted of four subcompartments: plasma, red blood cells (together forming the vascular space), interstitial fluid, and cellular space. A permeation barrier exists between the vascular space and the interstitial fluid, and between the interstitial fluid and the cellular space. The organ-to-plasma partition coefficients were determined using drug physicochemical properties based on methods described by Rodgers *et al.*²⁰ and Rodgers and Rowland.²¹

Drug-specific information from the literature included physicochemical properties and clearance pathways of the drug (Table 1). Mass balance studies with radiolabeled *i.v.* fluconazole indicated that 91% of fluconazole was eliminated in the urine, with 80% as unchanged drug, 2% was eliminated in the feces, and 7% was not recovered.²² As a result, the model assumed 15% of the plasma clearance of fluconazole was due to hepatic metabolism and 85% to renal elimination. Fluconazole is highly reabsorbed in the renal tubule. For drugs that are reabsorbed, PK Sim requires an input for the fraction of tubular reabsorption by calculating the glomerular filtration rate (GFR) fraction as follows:

$$\text{GFR Fraction} = \frac{\text{Empiric CL}_R}{\text{Expected CL}_R} \quad (1)$$

where Empiric CL_R equals the renal plasma clearance reported in the literature.²³ Expected CL_R is the renal plasma

Table 1 Fluconazole drug-dependent parameters representing physicochemical properties and elimination pathways

Parameter	Reported value	Optimized value
Physicochemical properties		
Lipophilicity (LogP)	0.4 ⁴⁴	1.1
Plasma binding protein	Alpha-1 acid glycoprotein ^{32,33}	
Fraction unbound (%)	89 ⁴⁵	
Molecular weight (g/mol)	306.27 ⁴⁴	
Compound type/pKa	Weak base/2.56 ⁴⁴	
Charge	Neutral ⁴⁴	
Blood/plasma ratio	1.0 ²⁷	
Metabolism and elimination		
Fraction of tubular reabsorption (GFR fraction)	0.16 (0.15–0.18) ^{27,28}	0.17
UGT2B7 specific CL (l/minute)	0.0052 (0.0031–0.0073) ^{27,28}	0.005

CL, clearance; GFR, glomerular filtration rate.

clearance expected due to GFR if there was no reabsorption or tubular secretion (expected CL_R = fraction unbound × GFR = $f_u \times 110$ mL/minute). Metabolism was attributed to glucuronidation via UGT2B7, and unbound intrinsic clearance (CL_H^u) was calculated using hepatic clearance (CL_H).²⁴ The CL_H^u was assumed to be 15% of total empiric clearance.²³ A summary of the assumptions used in the model building process is included in Table S1. Plasma concentration vs. time profiles were generated using the initial model and compared with observed data from the literature (Adult Development Datasets, Table S2). Model parameters were optimized based on the observed data using the Monte Carlo simulation in the PK Sim parameter identification toolbox. The optimized model was used to generate population predictions of plasma concentration vs. time profiles for a virtual population of healthy adults ($n = 1,000$) created using the PK-Sim population module.²⁵ Interindividual variability of UGT2B7 expression was assumed to have log-normal distribution with a geometric SD of 1.34.²⁶ Fluconazole's unbound fraction (f_u) was assumed to have a normal distribution with an arithmetic SD of 7%.^{27,28} Optimized model predictions for the virtual population were compared first with the observed data from the Adult Development Datasets to determine whether the model met acceptance criteria (see PBPK Model Acceptance Criteria below). In order to evaluate the model performance, the optimized model predictions were compared with observed data from the literature that were not used in the model building process (Adult Validation Datasets, Table S2). After acceptance criteria were met, the model was scaled to children.

Pediatric PBPK model

Age dependencies in physiological parameters (e.g., body weight, organ weight, and blood flow) were included to scale the adult PBPK model to children according to the methods described by Edginton *et al.*¹⁴ Briefly, parameters were assigned for each simulated individual: age, race, gender, mean body weight, and height.¹⁹ Based on body

weight and height, organ weights and volumes were obtained from the International Commission on Radiological Protection database.¹⁹ Age-dependent blood flows for some organs were available in the literature.¹⁴ For the organs in which no data were available, the same percentage of cardiac output in adults was assumed. The ontogeny function of alpha-1-acid glycoprotein (AAG) was taken from Maharaj *et al.*²⁹ using Eq. 2 and assuming a coefficient of variation of 25%.

$$AAG_i = \frac{PNA^{0.735}}{11.53^{0.735} + PNA^{0.735}} \quad (2)$$

where AAG_i is the AAG concentration for individual i and PNA is postnatal age in days.

The method developed by Edginton *et al.*³⁰ was used to scale clearance processes. GFR was scaled to children by calculating the percentage of adult GFR expected in a child of a specific age, and adjusted for $f_{u(\text{child})}$:

$$CL_{GFR(\text{child})} = \frac{GFR_{(\text{child})}}{GFR_{(\text{adult})}} \times \frac{f_{u(\text{child})}}{f_{u(\text{adult})}} \times CL_{GFR(\text{adult})} \quad (3)$$

where $CL_{GFR(\text{child})}$ is the child's clearance due to GFR, $GFR_{(\text{child})}$ is the estimated GFR of the child, $GFR_{(\text{adult})}$ is the GFR in adults (assumed to be 110 mL/minute), and $CL_{GFR(\text{adult})}$ is the clearance due to GFR in adults. The $GFR_{(\text{child})}$ was calculated using a postmenstrual age model,³¹ and $f_{u(\text{child})}$ was estimated using an age-specific model considering plasma protein concentrations in children and the affinity of drugs for binding proteins.^{30,32} Reabsorption (GFR fraction) was assumed to have no ontogeny.

UGT2B7 clearance was scaled to children as follows:

$$CL'_{UGT2B7(\text{child g liver})} = OSF_{UGT2B7} \times CL'_{UGT2B7(\text{adult g liver})} \quad (4)$$

where $CL'_{UGT2B7(\text{child g liver})}$ is the scaled CL' due to UGT2B7 per gram of liver, OSF_{UGT2B7} is the ontogeny scaling factor for UGT2B7 as a function of age,³³ and $CL'_{UGT2B7(\text{adult g liver})}$ is the adult CL' due to UGT2B7.

In order to evaluate the performance of the pediatric PBPK model, model predictions were generated using a simulated population of infants ($N = 1,000$) created with the PK-Sim population module²⁵ and compared with raw data from a PK study of fluconazole in critically ill infants (Pediatric Validation Dataset, **Table S2**). The median (5th and 95th percentiles) area under the concentration-time curve (AUC_{0-24}) for these 13 children was 485 mg hour/L (350 and 664) and was calculated using compartmental methods as described in Piper *et al.*³⁴

ECMO PBPK model

The pediatric PBPK model was exported into MoBi where a new compartment reflecting the ECMO circuit was added. Flow into and out of the ECMO compartment was assigned by partitioning pulmonary blood, with 80% allocated to the ECMO compartment and 20% allocated to the lungs. The ECMO compartment was assigned a volume of 400 mL to reflect the standard volume of blood required to prime the ECMO circuit. Because *ex vivo* studies indicate that fluconazole is not adsorbed by the circuit,^{9,15} no additional

clearance parameter was added for the ECMO compartment. The ECMO PBPK model was exported from MoBi back into PK Sim where the edema disease state was added to the model. Because children on ECMO develop severe edema secondary to capillary leak syndrome, edema was added to the model by scaling the child's body weight by 30%, and assigning the resulting increase in volume to the interstitial space of all organ compartments.^{16,17} In addition the interstitial:plasma protein ratio was increased from the default value of 0.37 to 1 to account for equalization of proteins due to capillary leakage.³⁵ Using the ECMO edema model, population simulations were performed and evaluated by comparing model predictions with observed data from the previously published Fluconazole ECMO trial.¹⁰ To determine the optimal loading dose that achieves target exposures for fluconazole in children on ECMO, new simulations were performed using the ECMO PBPK model with distinct loading dose regimens for different age groups.³⁶

Assessment of dose-exposure relationship

Fluconazole is fungistatic and has a prolonged postantibiotic effect. Efficacy is associated with an AUC to minimum inhibitory concentration (AUC/MIC) ratio ≥ 50 .^{37,38} Assuming a MIC of 8 mg/L, based on the Clinical and Laboratory Standards Institute's sensitivity breakpoint for all *Candida* species, an AUC_{0-24} of 400 mg * hour/L achieves the target AUC/MIC ratio.³⁹ For treatment, a target minimum AUC_{0-24} of 400 mg * hour/L in 90% of children was chosen. In order to balance efficacy and safety, predicted exposures also were compared with maximum tolerated AUC_{0-24} (1,600 mg * hour/L) and peak plasma concentration (C_{max} 70 mg/L).⁴⁰

PBPK model acceptance criteria

The population predictability was assessed by generating a prediction interval (5th to 95th percentile) of drug concentrations for the population, and quantifying the number of observed concentrations that fell outside of the prediction interval. Because the goal of this model was to determine dosing, and because dosing is based on AUC, minimal bias in AUC estimates was desired. Model precision was assessed by calculating the fold error between PBPK predicted AUC and observed AUC.

$$\text{Fold Error} = \frac{AUC_{0-24} \text{ PBPK}}{AUC_{0-24} \text{ Observed}} \quad (5)$$

Parameters with 0.7–1.3 fold error were considered as reasonable predictions.¹⁴

Clinical PK data used in this publication were collected during the Fluconazole Loading Dose clinical trial (ClinicalTrials.gov #NCT00797420) and Fluconazole ECMO clinical trial (ClinicalTrials.gov #NCT01169402). Both study protocols were reviewed and approved by the Duke institutional review board.

RESULTS

Adult PBPK model

Lipophilicity, mean fraction of tubular reabsorption, and UGT2B7 specific clearance were optimized to 0.17, 1.1, and 0.005 L/minute, respectively (**Table 1, Table S1**) using Adult

Development Datasets (Table S2). Optimized adult PBPK model predictions vs. dose-normalized observed data from the two Model Development Datasets showed good agreement, with over 90% of the observed data within the 90% prediction interval of the simulated population concentrations (Figure 2). The predicted AUCs were within 5% of observed AUC (Table 2).

When optimized model predictions were compared with observed data from Adult Validation Datasets (i.e., data not used to build the model), over 90% of the observed data were within the 90% prediction interval of the model and predicted AUCs were within 8% of observed AUCs (Figure S1; Table 2). As such, the adult PBPK model was scaled to children.

Scaling to children

Pediatric simulations evaluating the recommended loading dose of 25 mg/kg^{34,41} showed good agreement between observed vs. predicted concentrations, with 74% (32/43) of the observed data within the 90% prediction interval of

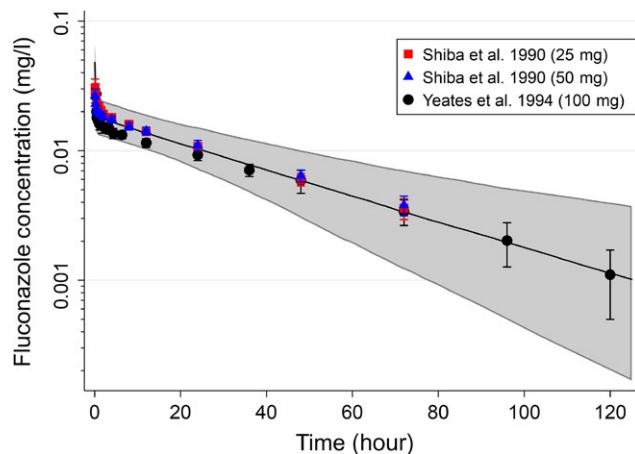


Figure 2 Adult optimized model. The physiologically based pharmacokinetic concentration-time model predictions for a dose of 1 mg. Solid black line represents the median predicted concentration; gray shaded area represents the 90% prediction interval; observed data from the Adult Development Datasets^{44,45} were dose-normalized to 1 mg and are represented by symbols (mean ± 90% confidence interval).

the simulated population concentrations (Figure 3). Nine of the 11 (82%) concentrations outside of the 90% prediction interval were from infants with renal dysfunction or severe edema. The observed AUC₀₋₂₄ estimate using compartmental modeling was 485 mg hour/L, and 84% of the individuals were above the target AUC₀₋₂₄ of 400 mg hour/L. The pediatric PBPK model predicted an AUC₀₋₂₄ of 513 mg hour/L (fold error 1.06) with 93% of simulated individuals achieving the target AUC₀₋₂₄ of 400 mg hour/L.

ECMO PBPK model

When the observed data from the Fluconazole ECMO trial were compared to the model predictions from the pediatric PBPK model, only 29% (12/42) of the observed data were within the 90% prediction interval (Figure 4a). Compared to the observed AUC₀₋₂₄ (371 mg hour/L) reported in the published population PK analysis,¹⁰ the AUC₀₋₂₄ was over-predicted (539 mg hour/L; 1.45 fold error). Adding the ECMO compartment to the pediatric PBPK model modestly improved predictions, although only 36% (15/42) of the observed data were within the 90% prediction interval (Figure 4b). The AUC₀₋₂₄ was still over-predicted, but to a lesser extent (487 mg hour/L; 1.31 fold error). The model over-predicted concentrations in the distribution phase. Thus, edema was incorporated into the model. After adding the edema disease state, 74% (31/42) of the observed data were within the 90% model prediction interval (Figure 4c). The PBPK predicted AUC₀₋₂₄ for a loading dose of 25 mg/kg for the ECMO PBPK model was 369 mg hour/L, which equated to a 0.99 fold error compared to the observed AUC₀₋₂₄ of 371 mg hour/L.¹⁰

Based on the precision of AUC estimates, the ECMO PBPK model was used to simulate multiple dosing regimens and identify the optimal loading dose for each age group. The following age-dependent loading doses were found to achieve the target AUC₀₋₂₄ in ≥90% of simulated children on ECMO in the first 24 hours of therapy: neonates (0–28 days) 30 mg/kg, infants (29 days to <2 years) 35 mg/kg, children (2 years to <6 years) 35 mg/kg, school-age children (6 to <12 years) 35 mg/kg, and adolescents 30 mg/kg (Figure 5a).

Because complicated dosing regimens are often difficult to implement, the ECMO PBPK model was also used to simulate exposures after a loading dose of 35 mg/kg for all age cohorts (Figure 5b). This approach achieved the

Table 2 Observed versus PBPK predicted AUCs for adult studies used in model development and validation

Population	N	Dose (mg)	Observed AUC (mg hour/L)	PBPK predicted AUC (mg hour/L)	Fold error
Adult development datasets					
Healthy volunteers ⁴⁴	10	100	73 ^a	77	1.05
Healthy volunteers ⁴⁵	8	50	34 ^b	35	1.03
		25	17 ^b	17	1.00
Adult validation datasets					
Healthy volunteers ⁴⁶	10	50	39 ^a	36	0.92
Healthy volunteers ⁴⁷	10	100	32 ^c	33	1.03

One of the adult validation datasets⁴⁸ did not report AUC and was not included in this table. AUC time intervals reported in the Adult Development and Validation Datasets varied by study, so the PBPK model generated a corresponding AUC for each study: ^aAUC_{0-∞} after a single dose. ^bAUC₀₋₇₂ after a single dose. ^cAUC₀₋₂₄ after a single dose.

AUC, area under the concentration-time curve; PBPK, physiologically based pharmacokinetic.

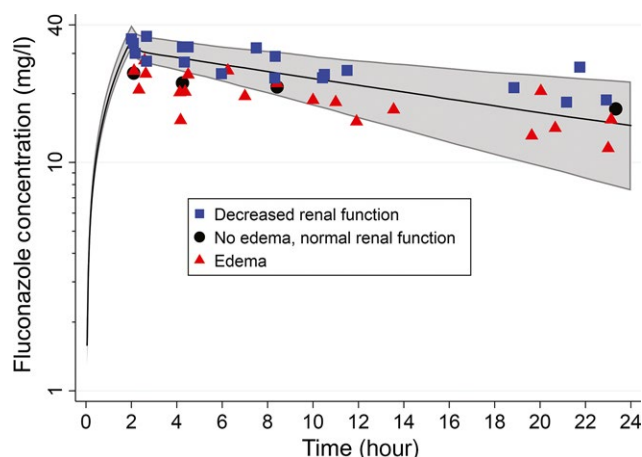


Figure 3 Pediatric physiologically based pharmacokinetic model predictions and observed data from critically ill infants.³⁴ All infants received a single 25 mg/kg loading dose. Solid black line is median predicted concentration; gray shaded area represents the 90% prediction interval; observed data are represented by symbols. For the observed data, the diagnosis of edema was based on physical examination. Renal dysfunction was defined as estimated glomerular filtration rate ≤ 50 mL/minute, the rate at which fluconazole dose modification is recommended.

target AUC_{0-24} in $\geq 98\%$ of simulated children on ECMO in the first 24 hours of therapy. Target attainment rates by cohort ranged from 96% in infants to $>99\%$ in adolescents. No simulated child had an AUC_{0-24} or C_{max} greater than the safety threshold values of 1,600 mg hour/L and 70 mg/L, respectively.⁴⁰

DISCUSSION

The critically ill child, especially with extracorporeal support, represents a population in which a conventional pediatric study paradigm for dose selection does not apply, and a PBPK approach can present a viable alternative. However, this approach has never been used in this population. In the present study, an established workflow for PBPK-based scaling from adults to children was used, and then the ECMO device and disease state effects (i.e., edema) were added to reasonably characterize exposure observed in children on ECMO.

The healthy adult model was scaled to children, and then the healthy infant model was used to predict exposures in critically ill infants. In the process of scaling to children, drug-specific inputs used in the optimized adult PBPK model were held constant, and system-specific inputs were scaled to the population of interest. The pediatric PBPK model only captured 74% of the observed data for critically ill infants, but this was expected because the model was based on healthy infants. Critically ill children have more variability in exposure due to disease. An examination of the data that fell below the 90% prediction interval revealed that 8 of the 10 observations (80%) were from children who had just undergone cardiac surgery and had substantial edema and inflammation, which would result in a higher volume of distribution and lower initial fluconazole exposure.^{16,42,43} Similarly, of the three concentrations that were greater than

the 90% prediction interval, all (100%) came from infants with a GFR ≤ 50 mL/minute. Decreased GFR for fluconazole, which undergoes renal clearance, resulted in decreased CL and higher than expected exposures. Adjustments in the model depend on the purpose of the model. For example, if the purpose is to predict dosing in children after cardiac surgery, then the model parameters need to be adjusted for the edema disease state to better describe the altered physiology in that population. The purpose of the pediatric PBPK model was to build the ECMO PBPK model and predict dosing in children on ECMO. Before adding an ECMO compartment, confidence in the scaling process from adults to children needed to be established. The pediatric PBPK model was deemed acceptable for developing the ECMO PBPK model because it explained the majority of concentrations that fell outside the 90% prediction interval, and because the observed and PBPK-predicted AUC_{0-24} values showed close agreement.

Observed data from the Fluconazole ECMO trial indicated that exposures were substantially lower in infants on ECMO compared to critically ill infants not on ECMO. As a result, the pediatric PBPK model overpredicted exposure in children on ECMO. Adding the ECMO compartment only lowered exposure by $\sim 5\%$. This was expected because the only direct impact of ECMO was the addition of 400 mL of blood required to prime the ECMO circuit. That effect is likely to be even less for older children where the ratio of prime volume (400 mL) to native blood volume is much lower. The ECMO PBPK model suggests that the bigger impact on fluconazole exposure may be attributed to edema, which is common in infants on ECMO. ECMO support results in inflammation and subsequent capillary leakage and edema.^{16,42,43} In addition, ongoing fluid resuscitation can result in a substantial increase in interstitial fluid volume.¹⁶ When the interstitial fluid volume in the ECMO PBPK model was increased, predicted exposure showed good agreement with the observed data.

The edema disease state was based on the assumption that edema caused a 30% increase in body weight, and that the increase in the volume was added to the interstitial compartment of each organ. A 30% increase in body weight is on the upper end of what would be expected.^{16,42,43} The model predictions were sensitive to the extent of edema. If a 10% increase in body weight was assumed, the model-predicted AUC_{0-24} after 25 mg/kg was 420 mg hour/L (1.13 fold error). We acknowledge that the assumptions about edema are simplistic. The trials that provided PK data for model evaluation were not designed to measure edema. In order to improve accuracy of this parameter, future studies should capture both the extent of edema in each individual and other factors, such as ongoing fluid resuscitation and biomarkers of inflammation that can lead to altered PK.

One of the advantages of PBPK modeling is the ability to predict dosing across the pediatric age spectrum. In infants on ECMO, our previous population PK model of fluconazole predicted that a loading dose of 35 mg/kg followed by 12 mg/kg daily was needed to achieve and maintain adequate exposure within 24 hours.¹⁰ Because that model was developed using data from infants, it was not known whether those dosing recommendations could be applied to older

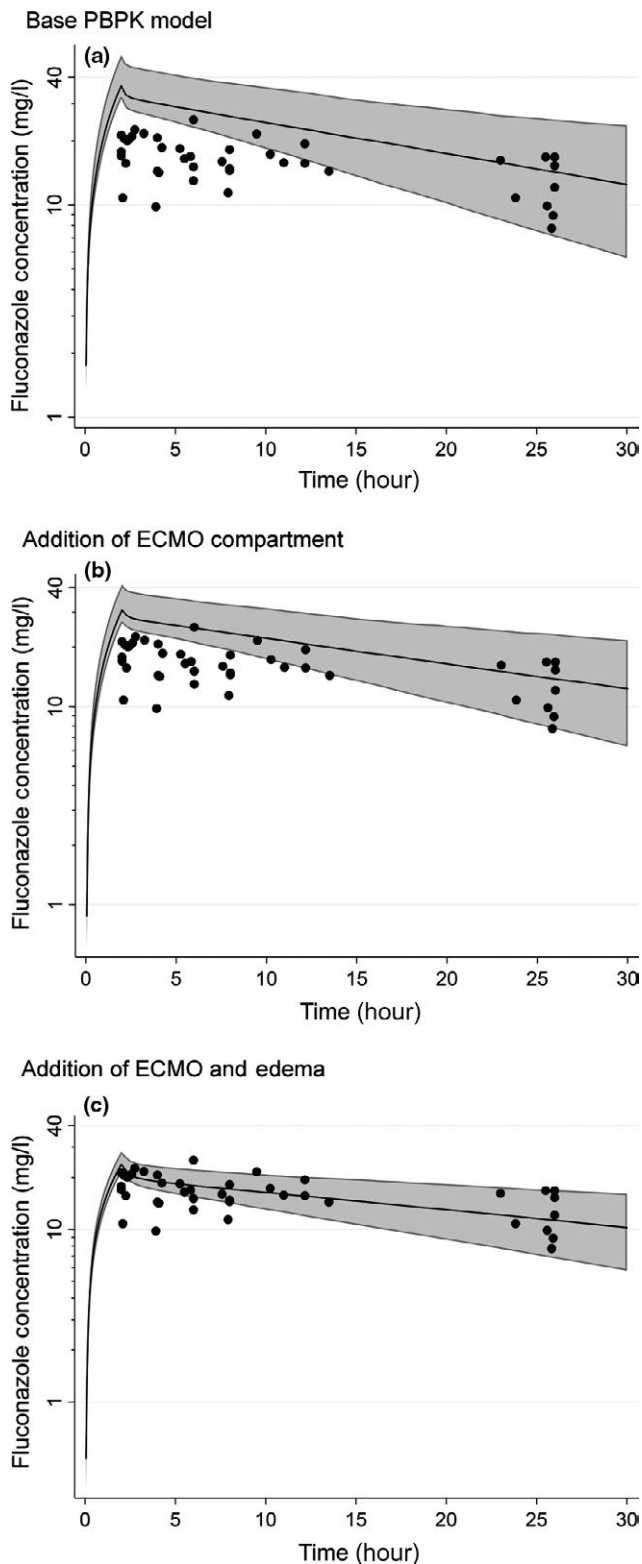


Figure 4 The extracorporeal membrane oxygenation (ECMO) physiologically based pharmacokinetic (PBPK) model development. The PBPK model predictions and observed data were based on a loading dose of 25 mg/kg in infants. (a) Base PBPK model: pediatric PBPK model predictions vs. observed concentrations in infants on ECMO. (b) Addition of ECMO compartment to the pediatric PBPK model. (c) Addition of the ECMO compartment and incorporation of edema to the pediatric PBPK model.

children. By accounting for the developmental changes in body size and physiology as children age, the current ECMO PBPK model was able to predict the optimal loading dose for each age group. However, the optimal regimen may be too complicated for clinical implementation. Choosing a single weight-based dose for all children involves balancing the consequences of underexposure with the risk of toxicity due to overexposure. Fluconazole is safe up to a C_{max} of 70 mg/L and a maximum AUC_{0-24} of 1,600 mg * hour/L.⁴⁰ Based on the wide therapeutic index and because the consequences of an inadequately treated fungal infection in a child on ECMO are devastating, dosing should target a higher exposure to ensure that all children are adequately treated. A loading dose of 35 mg/kg for all children achieved the therapeutic exposure within 24 hours in over 99% of simulated children; importantly, no simulated children exceeded the known safety thresholds. Based on this, a fluconazole loading dose of 35 mg/kg is recommended for all children with suspected or confirmed fungal infection who are supported with ECMO.

The successful translation of ECMO *ex vivo* results into dosing recommendations using PBPK modeling has several implications. First, the workflow of PBPK model development-validation-application presented here (Figure 1) can be generalized to prospectively predict drug PK in a specific population undergoing other forms of extracorporeal support (e.g., dialysis). Depending on how existing disease was characterized during model development and validation (steps 1 and 2), a PBPK model with an adequately parameterized extracorporeal device compartment can be used to simulate drug PK under various untested clinical situations to either aid dose selection for a smaller, more efficient confirmatory trial or to ultimately replace such trials (step 3). Second, when new extracorporeal technology is introduced, *ex vivo* experiments can be performed to determine the interaction of the drug (e.g., fluconazole) with the new circuit. If interaction is different, the extracorporeal compartment can be reparameterized and new model-based dosing recommendations derived. In conclusion, the ECLS-PBPK method described in this study should provide an approach to dose determination in this difficult to study population that provides needed flexibility to account for different and evolving extracorporeal circuit components and reduces the number of children enrolled in clinical trials.

Supporting Information

Supplementary information accompanies this paper on the *CPT: Pharmacometrics & Systems Pharmacology* website. (www.psp-journal.com)

Figure S1. Adult model validation.

Table S1. Assumptions used in the model building process.

Table S2. Studies used in model development and evaluation.

Appendix S1. Model Code – Fluconazole PBPK Model Development. Summary of model building process and parameters. Model Code – MoBi File. MoBi file with ECMO compartment and edema.

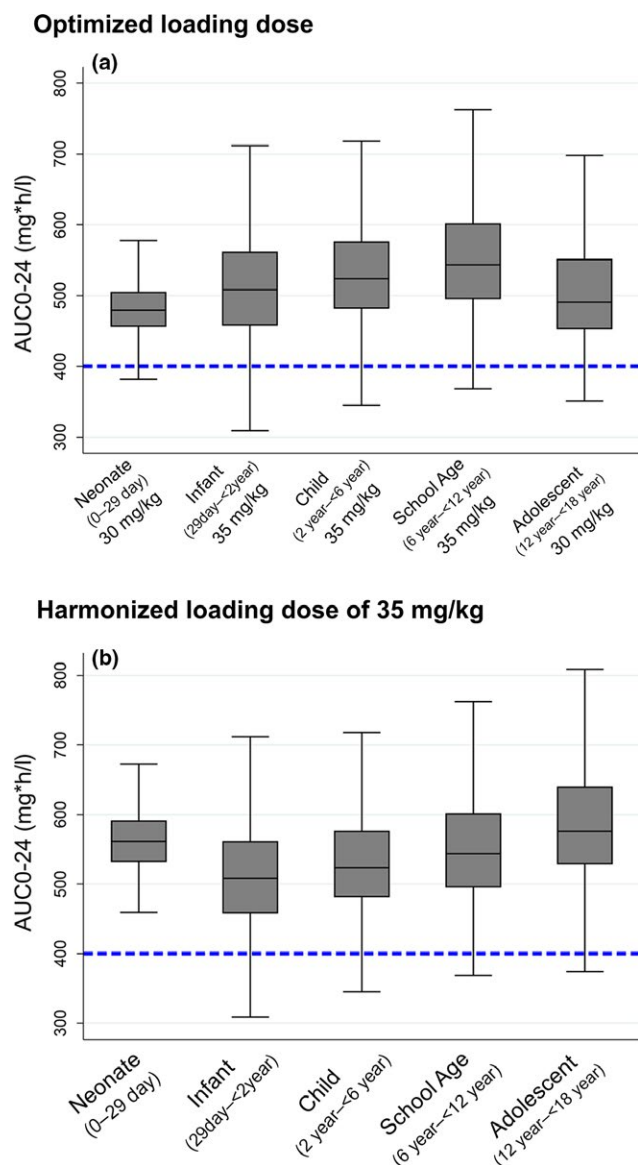


Figure 5 The extracorporeal membrane oxygenation (ECMO) physiologically based pharmacokinetic (PBPK) model-predicted optimized fluconazole loading dosing and exposure in children on ECMO across the pediatric age spectrum. Solid line represents the median, box represents interquartile range, and whiskers represent 90% prediction interval. Dosing achieved the target area under the concentration-time curve (AUC)₀₋₂₄ (>400 mg hour/L, blue dashed line) in ≥90% of simulated children on ECMO in the first 24 hours of therapy. (a) Optimized loading dose. (b) Harmonized loading dose using 35 mg/kg loading dose.

Acknowledgments. The authors wish to thank Martin Hobe, Tobias Kanacher, Michael Block, Thomas Wendl, and Sebastien Frechen from Bayer Technology Services for their helpful discussions regarding PK Sim and MoBi software-related questions.

Funding. This work was funded under 1K23HD075891 (PI Watt), 5K12HD047349 (PI Dean), and 2K24HD058735 (PI Benjamin). K.M.W. receives support from the Pediatric Critical Care and Trauma Scientist

Development Program (5K12HD047349) and the Eunice Kennedy Shriver National Institute of Child Health and Human Development (1K23HD075891, 2K24HD058735). M.C.-W. receives support for research from the National Institutes of Health (NIH; 1R01-HD076676-01A1), the National Center for Advancing Translational Sciences of the NIH (UL1TR001117), the National Institute of Allergy and Infectious Disease (NIAID) (HHSN2722015000061 and HHSN2722013000171), NICHD (HHSN2752010000031), the Biomedical Advanced Research and Development Authority (BARDA) (HHSO100201300009C), the non-profit organization Thrasher Research Fund (www.thrasherresearch.org), and industry for drug development in adults and children (www.dcri.duke.edu/research/coi.jsp). At the time of their contributions to this work J.S.B. and P.Z. were at Children's Hospital of Philadelphia and the US Food and Drug Administration, respectively, and have no funding to report. M.S. has no funding to report. K.L.R.B. was supported, in part, by funding from the NIH through award numbers R01 GM041935 and R35 GM122576 from the National Institute of General Medical Sciences. A.N.E. receives support for research from the NIH (1R01HD076676-01A1, 1K23HD075891). Software: prior to becoming open-source software, Bayer Technology Services provided the modeling software (PK Sim and MoBi) used in the analysis free of charge under an academic license to Duke University.

Conflict of Interest. As an Associate Editor for *CPT: Pharmacometrics & Systems Pharmacology*, P.Z. was not involved in the review or decision process for this paper. The authors have no conflicts of interest related to this manuscript.

Author Contributions. K.M.W., M.C.-W., K.L.R.B., and A.N.E. wrote the manuscript. K.M.W., M.C.-W., J.S.B., P.Z., K.L.R.B., and A.N.E. designed the research. K.M.W., M.C.-W., J.S.B., P.Z., K.L.R.B., and A.N.E. performed the research. K.M.W., M.C.-W., M.S., P.Z., K.L.R.B., and A.N.E. analyzed the data.

Informed Consent. Informed consent and assent when applicable was obtained from all participants enrolled in the clinical trials who contributed clinical PK data used in this study.

1. Preston, T.J., Hodge, A.B., Riley, J.B., Leib-Sargel, C. & Nicol, K.K. In vitro drug adsorption and plasma free hemoglobin levels associated with hollow fiber oxygenators in the extracorporeal life support (ECLS) circuit. *J. Extra Corpor. Technol.* **39**, 234-237 (2007).
2. Harthan, A.A., Buckley, K.W., Heger, M.L., Fortuna, R.S. & Mays, K. Medication adsorption into contemporary extracorporeal membrane oxygenator circuits. *J. Pediatr. Pharmacol. Ther.* **19**, 288-295 (2014).
3. Buck, M.L. Pharmacokinetic changes during extracorporeal membrane oxygenation: implications for drug therapy of neonates. *Clin. Pharmacokinet.* **42**, 403-417 (2003).
4. Kozik, D.J. & Tweddell, J.S. Characterizing the inflammatory response to cardiopulmonary bypass in children. *Ann. Thorac. Surg.* **81**, S2347-S2354 (2006).
5. McLlwain, R.B. et al. Plasma concentrations of inflammatory cytokines rise rapidly during ECMO-related SIRS due to the release of preformed stores in the intestine. *Lab. Invest.* **90**, 128-139 (2010).
6. Many, M., Soroff, H.S., Birtwell, W.C., Giron, F., Wise, H. & Deterling, R.A. Jr. The physiologic role of pulsatile and nonpulsatile blood flow. II. Effects on renal function. *Arch. Surg.* **95**, 762-767 (1967).
7. Cohen, P., Collart, L., Prober, C.G., Fischer, A.F. & Blaschke, T.F. Gentamicin pharmacokinetics in neonates undergoing extracorporeal membrane oxygenation. *Pediatr. Infect. Dis. J.* **9**, 562-566 (1990).
8. Amaker, R.D., DiPiro, J.T. & Bhatia, J. Pharmacokinetics of vancomycin in critically ill infants undergoing extracorporeal membrane oxygenation. *Antimicrob. Agents Chemother.* **40**, 1139-1142 (1996).
9. Shekar, K. et al. Protein-bound drugs are prone to sequestration in the extracorporeal membrane oxygenation circuit: results from an ex vivo study. *Crit. Care* **19**, 164 (2015).

10. Watt, K.M. *et al.* Fluconazole population pharmacokinetics and dosing for prevention and treatment of invasive Candidiasis in children supported with extracorporeal membrane oxygenation. *Antimicrob. Agents Chemother.* **59**, 3935–3943 (2015).
11. Wildschut, E.D., Ahsman, M.J., Allegaert, K., Mathot, R.A. & Tibboel, D. Determinants of drug absorption in different ECMO circuits. *Intensive Care Med.* **36**, 2109–2116 (2010).
12. Bizzarro, M.J., Conrad, S.A., Kaufman, D.A. & Rycus, P. Infections acquired during extracorporeal membrane oxygenation in neonates, children, and adults. *Pediatr. Crit. Care Med.* **12**, 277–281 (2010).
13. Gardner, A.H. *et al.* Fungal infections and antifungal prophylaxis in pediatric cardiac extracorporeal life support. *J. Thorac. Cardiovasc. Surg.* **143**, 689–695 (2011).
14. Edginton, A.N., Schmitt, W. & Willmann, S. Development and evaluation of a generic physiologically based pharmacokinetic model for children. *Clin. Pharmacokinet.* **45**, 1013–1034 (2006).
15. Watt, K.M. *et al.* Antifungal extraction by the extracorporeal membrane oxygenation circuit. *J. Extra Corpor. Technol.* **49**, 150–159 (2017).
16. Anderson, H.L. 3rd, Coran, A.G., Drongowski, R.A., Ha, H.J. & Bartlett, R.H. Extracellular fluid and total body water changes in neonates undergoing extracorporeal membrane oxygenation. *J. Pediatr. Surg.* **27**, 1003–1007 (1992); discussion 1007–1008.
17. Vrancken, S.L. *et al.* Influence of volume replacement with colloids versus crystalloids in neonates on venoarterial extracorporeal membrane oxygenation on fluid retention, fluid balance, and ECMO runtime. *ASAIO J.* **51**, 808–812 (2005).
18. Statistics NCFH. *Third National Health and Nutrition Examination Survey (NHANES III)* (Statistics NCFH, Hyattsville, MD, 1997).
19. ICRP. Basic anatomical and physiological data for use in radiological protection reference values. *Ann. ICRP* **32**, 3–4 (2002).
20. Rodgers, T., Leahy, D. & Rowland, M. Physiologically based pharmacokinetic modeling 1: predicting the tissue distribution of moderate-to-strong bases. *J. Pharm. Sci.* **94**, 1259–1276 (2005).
21. Rodgers, T. & Rowland, M. Physiologically based pharmacokinetic modelling 2: predicting the tissue distribution of acids, very weak bases, neutrals and zwitterions. *J. Pharm. Sci.* **95**, 1238–1257 (2006).
22. Brammer, K.W., Coakley, A.J., Jezequel, S.G. & Tarbit, M.H. The disposition and metabolism of [¹⁴C]fluconazole in humans. *Drug Metab. Dispos.* **19**, 764–767 (1991).
23. Debruyne, D. & Ryckelynck, J.P. Clinical pharmacokinetics of fluconazole. *Clin. Pharmacokinet.* **24**, 10–27 (1993).
24. Bourcier, K. *et al.* Investigation into UDP-glucuronosyltransferase (UGT) enzyme kinetics of imidazole- and triazole-containing antifungal drugs in human liver microsomes and recombinant UGT enzymes. *Drug Metab. Dispos.* **38**, 923–929 (2010).
25. Willmann, S. *et al.* Development of a physiology-based whole-body population model for assessing the influence of individual variability on the pharmacokinetics of drugs. *J. Pharmacokinet. Pharmacodyn.* **34**, 401–431 (2007).
26. Sim, S.M., Back, D.J. & Breckenridge, A.M. The effect of various drugs on the glucuronidation of zidovudine (azidothymidine; AZT) by human liver microsomes. *Br. J. Clin. Pharmacol.* **32**, 17–21 (1991).
27. Arredondo, G., Calvo, R., Marcos, F., Martinez-Jorda, R. & Suarez, E. Protein binding of itraconazole and fluconazole in patients with cancer. *Int. J. Clin. Pharmacol. Ther.* **33**, 449–452 (1995).
28. Arredondo, G., Martinez-Jorda, R., Calvo, R., Aguirre, C. & Suarez, E. Protein binding of itraconazole and fluconazole in patients with chronic renal failure. *Int. J. Clin. Pharmacol. Ther.* **32**, 361–364 (1994).
29. Maharaj, A.R., Gonzalez, D., Cohen-Wolkowicz, M., Hornik, C.P. & Edginton, A.N. Improving pediatric protein binding estimates: an evaluation of alpha1-acid glycoprotein maturation in healthy and infected subjects. *Clin. Pharmacokinet.* **57**, 577–589 (2018).
30. Edginton, A.N., Schmitt, W., Voith, B. & Willmann, S. A mechanistic approach for the scaling of clearance in children. *Clin. Pharmacokinet.* **45**, 683–704 (2006).
31. Rhodin, M.M. *et al.* Human renal function maturation: a quantitative description using weight and postmenstrual age. *Pediatr. Nephrol.* **24**, 67–76 (2009).
32. McNamara, P.J. & Alcorn, J. Protein binding predictions in infants. *AAPS PharmSci* **4**, E4 (2002).
33. Meyer, M., Schneckener, S., Ludewig, B., Kuepfer, L. & Lippert, J. Using expression data for quantification of active processes in physiologically based pharmacokinetic modeling. *Drug Metab. Dispos.* **40**, 892–901 (2012).
34. Piper, L. *et al.* Fluconazole loading dose pharmacokinetics and safety in infants. *Pediatr. Infect. Dis. J.* **30**, 375–378 (2011).
35. Radke, C. *et al.* Development of a physiologically based pharmacokinetic modeling approach to predict the pharmacokinetics of vancomycin in critically ill septic patients. *Clin. Pharmacokinet.* **56**, 759–779 (2017).
36. Wade, K.C. *et al.* Fluconazole dosing for the prevention or treatment of invasive candidiasis in young infants. *Pediatr. Infect. Dis. J.* **28**, 717–723 (2009).
37. Andes, D. & van Ogtrop, M. Characterization and quantitation of the pharmacodynamics of fluconazole in a neutropenic murine disseminated candidiasis infection model. *Antimicrob. Agents Chemother.* **43**, 2116–2120 (1999).
38. Clancy, C.J., Yu, V.L., Morris, A.J., Snyderman, D.R. & Nguyen, M.H. Fluconazole MIC and the fluconazole dose/MIC ratio correlate with therapeutic response among patients with candidemia. *Antimicrob. Agents Chemother.* **49**, 3171–3177 (2005).
39. Pai, M.P., Turpin, R.S. & Garey, K.W. Association of fluconazole area under the concentration-time curve/MIC and dose/MIC ratios with mortality in nonneutropenic patients with candidemia. *Antimicrob. Agents Chemother.* **51**, 35–39 (2007).
40. Anaissie, E.J. *et al.* Safety, plasma concentrations, and efficacy of high-dose fluconazole in invasive mold infections. *J. Infect. Dis.* **172**, 599–602 (1995).
41. Bradley, J.S. & Nelson, J.D., eds. *Nelson's Pediatric Antimicrobial Therapy 22nd edn.* (American Academy of Pediatrics, Itasca, IL, 2016).
42. Butler, J. *et al.* Acute-phase responses to cardiopulmonary bypass in children weighing less than 10 kilograms. *Ann. Thorac. Surg.* **62**, 538–542 (1996).
43. Seghaye, M.C. *et al.* Inflammatory reaction and capillary leak syndrome related to cardiopulmonary bypass in neonates undergoing cardiac operations. *J. Thorac. Cardiovasc. Surg.* **112**, 687–697 (1996).
44. Shiba, K., Saito, A. & Miyahara, T. Safety and pharmacokinetics of single oral and intravenous doses of fluconazole in healthy subjects. *Clin. Ther.* **12**, 206–215 (1990).
45. Yeates, R.A., Ruhnke, M., Pfaff, G., Hartmann, A., Trautmann, M. & Sarnow, E. The pharmacokinetics of fluconazole after a single intravenous dose in AIDS patients. *Br. J. Clin. Pharmacol.* **38**, 77–79 (1994).
46. Brammer, K.W., Farrow, P.R. & Faulkner, J.K. Pharmacokinetics and tissue penetration of fluconazole in humans. *Rev. Infect. Dis.* **12**(suppl. 3), S318–S326 (1990).
47. Brammer, K.W. & Tarbit, M.H.. A review of the pharmacokinetics of fluconazole (UK-49,858) in laboratory animals and man. In *Recent Trends in the Discovery, Development and Evaluation of Antifungal Agents* (ed. Fromtling, R.A.) 141–150 (J.R. Prous Science Publishers, Barcelona, 1987).
48. Foulds, G., Wajszczuk, C., Weidler, D.J., Garg, D.J. & Gibson, P. Steady state parenteral kinetics of fluconazole in man. *Ann. NY Acad. Sci.* **544**, 427–430 (1988).

© 2018 The Authors CPT: *Pharmacometrics & Systems Pharmacology* published by Wiley Periodicals, Inc. on behalf of the American Society for Clinical Pharmacology and Therapeutics. This is an open access article under the terms of the Creative Commons Attribution-NonCommercial License, which permits use, distribution and reproduction in any medium, provided the original work is properly cited and is not used for commercial purposes.